Clinical and Experimental Nephrology
https://doi.org/10.1007/s10157-019-01689-7

ORIGINAL ARTICLE

Low-energy extracorporeal shock wave ameliorates ischemic acute kidney injury in rats

Mai Yoshida[1] · Takashi Nakamichi[1] · Takefumi Mori[1] · Kenta Ito[2] · Hiroaki Shimokawa[2] · Sadayoshi Ito[1]

Received: 5 November 2017 / Accepted: 2 January 2019

Abstract

Background Low-energy extracorporeal shock wave (SW) improves ventricular function in ischemic cardiomyopathy through the upregulation of vascular endothelial growth factor (VEGF). VEGF is known to play important roles in acute kidney injury (AKI), and the present study investigates the efficacy of SW for AKI by renal ischemia–reperfusion (I/R) injury.

Methods Male 8-week-old Sprague–Dawley rats were divided into the following groups: SW-treated I/R group (I/R-SW), untreated I/R group (I/R), and Sham group. To induce I/R, the left renal pedicles were clamped for 45 min. The I/R-SW group was treated with SW to both kidneys on the immediate postoperative period (day 0), days 1, 2, 7, 8, 9, 14, 15, and 16. Rats were killed on day 2 and day 20 to determine histology, renal function, and *Vegf* family mRNA expression.

Results Plasma creatinine on day 2 was significantly lower in the I/R-SW group than in the I/R group. Light microscopy revealed significantly lower tubular injury scores for the outer medulla in the I/R-SW group than in the I/R group. Podoplanin-positive lymphatic vessels were significantly increased in the left (affected side) outer medulla in the I/R-SW group on day 20. The expression levels of *Vegf* in the right (intact side) cortex were significantly higher in the I/R-SW group than in the I/R group on day 2.

Conclusion Shock wave ameliorated renal tubular injury and renal function in AKI model, through the stimulation of *Vegf* family expression and lymphangiogenesis. SW may be effective as a non-invasive treatment for ischemic AKI.

Keywords Ischemic acute kidney injury · Shock wave · Vascular endothelial growth factor · Lymphangiogenesis

Introduction

Acute kidney injury (AKI) is characterized by a rapid decline in the glomerular filtration rate and a prospective study from Japan reported that the incidence of AKI requiring renal replacement therapy was 13.3 cases/100,000 persons/year, and the in-hospital mortality rate was 47.1% [1]. Accordingly, there is a clinical need for novel treatment strategies for AKI.

A number of systemic disorders (e.g., sepsis, cardiogenic shock), major surgery, and nephrotoxic drugs are known to cause ischemic AKI [2], which is pathologically characterized by acute tubular injury. Renal ischemia induces vascular endothelial growth factor (VEGF) secretion. VEGF is normally localized in podocytes and tubular epithelial cells in the human kidney [3, 4] and has been shown to mediate recovery from AKI through the stimulation of microvascular proliferation, vascular dilatation, and cell survival.

Extracorporeal shock wave treatment has been traditionally used for urolithiasis. Since 2000s, we have demonstrated that low-energy extracorporeal shock wave (SW), which energy density is approximately 10% for urolithiasis, induced therapeutic angiogenesis and improved myocardial ischemia through the upregulation of VEGF and nitric oxide (NO) expression in a model of porcine ischemic cardiomyopathy [5] and in patients with severe ischemic heart diseases [6, 7]. Furthermore, basic and clinical research studies have reported the efficacy of SW in treating a number of other conditions, including peripheral artery disease [8], acute myocardial infarction [9–11], lymphedema [12], and spinal cord injury [13]. For AKI, some reports showed that

✉ Takashi Nakamichi
tnakamichi@med.tohoku.ac.jp

[1] Division of Nephrology, Endocrinology and Vascular Medicine, Tohoku University Graduate School of Medicine, 1-1 Seiryo-machi, Aoba-ku, Sendai 980-8574, Japan

[2] Department of Cardiovascular Medicine, Tohoku University Graduate School of Medicine, 1-1 Seiryo-machi, Aoba-ku, Sendai 980-8574, Japan

Published online: 07 January 2019

ultrasound, which was similar to SW, prevented murine renal I/R by anti-inflammatory pathway [14, 15]. However, there was no research about the relationship between SW and AKI through VEGF pathway.

In the present study, we hypothesized that SW is effective in ameliorating renal injury in ischemic AKI through the stimulation of VEGF activity in a rodent model of ischemic AKI.

Materials and methods

Animals

Male 8-week-old Sprague–Dawley rats (purchased from Japan SLC, Inc., Hamamatsu, Japan) were housed in a 12-h light–dark cycle, provided standard chow (Nosan, Yokohama, Japan) and tap water ad libitum, and cared for in accordance with the principles and guidelines of the Japanese Ministry of the Environment.

Experimental design

We performed I/R surgery on day 0. Briefly, the rats were anesthetized by an intra-peritoneal injection of pentobarbital sodium (5 mg/100 g BW) and inhalation of sevoflurane. Following left flank incision, the left renal pedicles were clamped for 45 min and then declamped before wounds were closed. Rats were divided into the following three groups: SW-treated I/R group (I/R-SW, $n=13$), untreated I/R group (I/R, $n=12$), and the Sham group (Sham, $n=12$). The Sham group underwent left flank incisions only. Rats were killed on day 2 (I/R-SW, $n=8$; I/R, $n=7$; Sham, $n=6$) and day 20 (IR-SW, $n=5$; IR, $n=5$; Sham, $n=6$). The kidneys were harvested for renal volume, histological analysis, and real-time PCR studies. Simultaneously, blood was collected to measure creatinine concentration. The experimental design is shown in Fig. 1.

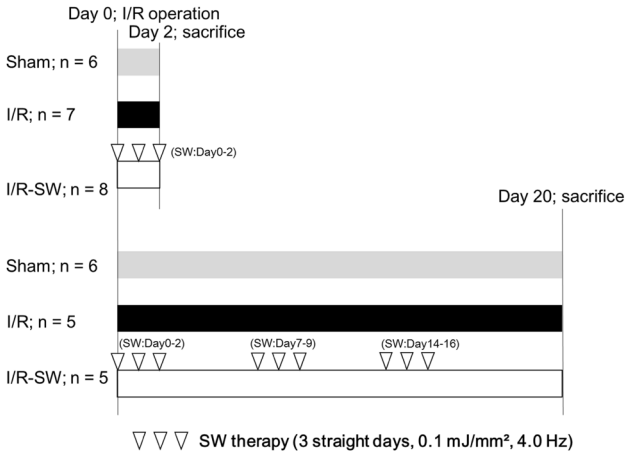

Fig. 1 Experimental design. The left renal pedicles were clamped for 45 min and then declamped before wounds were closed. Rats were divided into three groups: the Sham group (Sham, $n=12$), untreated I/R group (I/R, $n=12$), SW-treated I/R group (I/R-SW, $n=13$). The Sham group underwent skin incisions only. Rats were killed on day 2 (Sham, $n=6$; I/R, $n=7$; I/R-SW, $n=8$) and day 20 (Sham, $n=6$; IR, $n=5$; IR-SW, $n=5$). *SW* shock wave for both kidneys, *I/R* ischemia–reperfusion

Serological analyses

Blood was centrifuged (3000 rpm, 10 min, 4 °C) and the supernatant was collected as plasma. The plasma creatinine concentration was measured with biochemical automatic analyzer (UniCel DxC800; Beckman Coulter Inc, CA, USA).

SW therapy

Rats in the I/R-SW groups received SW therapy to both kidneys (two sites/kidney) on the immediate postoperative period (day 0), days 1, 2, 7, 8, 9, 14, 15, and 16. SW treatment consisted of 200 shocks with 0.1 mJ/mm^2 (positive energy flux density) per day for each kidney using a SW generator (DUOLITH SD1; Storz Medical AG, Tägerwilen, Switzerland). Settings were based on previous studies [5–13], in which maximal upregulation of VEGF expression was achieved.

Histological analysis

A part of the harvested renal tissue was fixed in 10% buffered neutral formalin (Wako, Tokyo, Japan), embedded in paraffin, and sectioned at a thickness of 2 μm. Sections from rats killed on day 2 and day 20 were examined under a light microscope following Elastica–Masson (EM) staining. A total of 20 sections (×400) from the cortex and outer medulla were randomly quantified for each animal. Tubular injuries were scored according to a previous study [16].

Immunohistochemistry

For immunohistochemical analyses, the kidney tissue was fixed, embedded, and sectioned in the same manner as for histological analyses. Sections from rats killed on day 2 were incubated with primary antibodies against α-smooth muscle actin (αSMA) (dilution of 1:100, DAKO A/S, Glostrup, Denmark), ED-1 (dilution of 1:100, AbD Serotec, Kidlington, UK), and Cleaved Caspase-3 (dilution of 1:200, Cell Signaling Technology, MA, USA) at 4 °C overnight. Sections from rats killed on day 20 were incubated with primary antibodies against αSMA, podoplanin (dilution of 1:100, Nichirei, Tokyo, Japan), and CD-31 (dilution of 1:200, Santa Cruz Biotechnology, TX, USA) at 4 °C overnight.

After washing with PBS, sections were then incubated with secondary antibodies at 37 °C for 30 min and washed in PBS. The chromogenic reaction was visualized using 3-3′-diaminobenzidine (Dojindo, Kumamoto, Japan). The αSMA, ED-1, and Cleaved Caspase-3-positive areas in each of the 20 sections (αSMA, ED-1: ×200, Cleaved Caspase-3: ×100) from the cortex and outer medulla were randomly quantified for each animal with a computer software Image J®. The number of podoplanin-positive vessels was counted from ten randomly selected sections of the cortex and outer medulla (×200). Lymphatic vessels in the vicinity of the interlobular arteries were not considered because they were physiologically present in the normal kidney [17].

Real-time PCR

A part of the renal tissue was stored in RNA later® (Ambion, Austin, TX, USA) to stabilize RNA. Total RNA was purified by RNeasy Plus Mini Kit (Qiagen, Hilden, Germany), according to the manufacturer's protocol. Real-time PCR to quantify the mRNA expression of *Vegf, Vegf-c, Vegfr-3, Vegf-a*, and *endothelial Nitric Oxide Synthase (eNOS)* was carried out using iScript™ One-Step RT-PCR Kit with SYBR® Green (Bio-Rad laboratories, CA, USA) on a CFX96 Touch™ real-time PCR detection system (Bio-Rad laboratories, CA, USA). The PCR conditions were as follows: 10 s at 95 °C, 30 s at 60 °C, and 10 s at 95 °C and 10 s at 60 °C for 40 cycles. Data were normalized to glutaraldehyde 3-phosphate dehydrogenase (*Gapdh*) expression. The primers were purchased from Takara Bio Inc. The list of primers is shown in Table 1.

Table 1 Primers used in real-time PCR analysis

Mouse gene	Sequence
Vegf	
Forward	ACGAAAGCGCAAGAAATCCC
Reverse	TTAACTCAAGCTGCCTCGCC
Vegf-c	
Forward	GCCAATCACACTTCCTGCCG
Reverse	CTGGCAGGTGTCTTCATCCAAC
Vegfr3	
Forward	ACTCCTGCCATACGCCACATC
Reverse	CTCAAACTCTTCTGAGGCCAGCACC
Vegf-a	
Forward	GTCCTCACTTGGATCCCGACA
Reverse	CCTGGCAGGCAAACAGACTTC
eNOS	
Forward	CTCAGGTTCTGTGTGTTTGGGCTGGG
Reverse	GGAGGACCCTCCGCCATCCACAGAG
Gapdh	
Forward	GGCACAGTCAAGGCTGAGAATG
Reverse	ATGGTGGTGAAGACGCCAGTA

Statistical analysis

Values are expressed as means and standard deviations. Data were analyzed using unpaired Student's *t* test or analysis of variance (ANOVA) and Tukey's HSD test by JMP® 11 (SAS Institute Inc., Cary, NC, USA). Results with $P < 0.05$ were considered statistically significant.

Results

Effects of SW on the left (affected side) kidney weight

After I/R surgery, the left (affected side) kidney weight significantly increased compared with the Sham group (I/R vs. Sham, 1.29 ± 0.03 vs. 0.98 ± 0.02; $P < 0.05$). The ratio of left (affected side) to right (intact side) kidney weight was significantly lower in the I/R-SW group than in the I/R group on day 2 (I/R-SW vs. I/R, 1.13 ± 0.05 vs. 1.29 ± 0.03; $P < 0.05$; Fig. 2a). This result suggested that SW attenuated congestion in the left (affected side) kidney. Differences in kidney weight between the three groups disappeared by day 20.

Serological analyses

Plasma creatinine concentrations in the I/R group were significantly elevated compared with the Sham group on day 2 (I/R vs. Sham, 0.43 ± 0.03 vs. 0.25 ± 0.01 mg/dL; $P < 0.05$). SW treatment significantly improved elevated creatinine (I/R-SW vs. I/R, 0.32 ± 0.02 vs. 0.43 ± 0.03 mg/dL; $P < 0.05$; Fig. 2b). Renal function in the I/R and I/R-SW groups on day 20 recovered to levels comparable to the Sham group.

Histological analyses

As shown in Fig. 3a, on day 2, most tubular epithelial cells were prominently necrotized and sloughed as debris in tubular lumen space in the left (affected side) kidney following I/R surgery. In addition, many inflammatory cells were observed in the interstitial area and many casts were seen in tubular lumen space. For the outer medulla of the left (affected side) kidney, tubular injury scores in the I/R-SW group were significantly lower than in the I/R group on day 2 (I/R-SW vs. I/R, 1.62 ± 0.20 vs. 2.04 ± 0.10; $P < 0.05$; Fig. 3b). Histological improvement was also observed in the cortical area of the left (affected side) kidney, although quantitatively assessed differences did not reach statistical difference. On day 20, the necrotized tubular epithelial cells and inflammatory cells decreased compared with day 2. Tubular

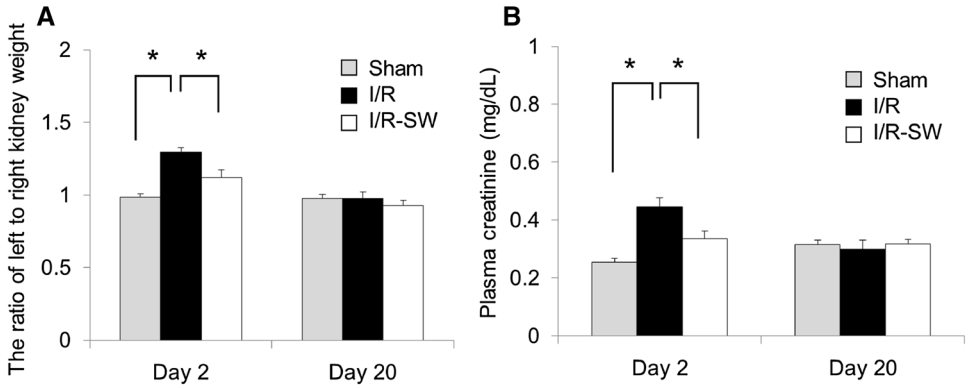

Fig. 2 Changes in renal volume and function. On day 2, **a** the ratio of left (affected side) to right (intact side) kidney weight and **b** plasma creatinine in the I/R-SW group were significantly lower than the I/R group. Data are expressed as means ± standard error. Tukey HSD test: $^{*}P < 0.05$. *I/R* ischemia–reperfusion, *SW* shock wave

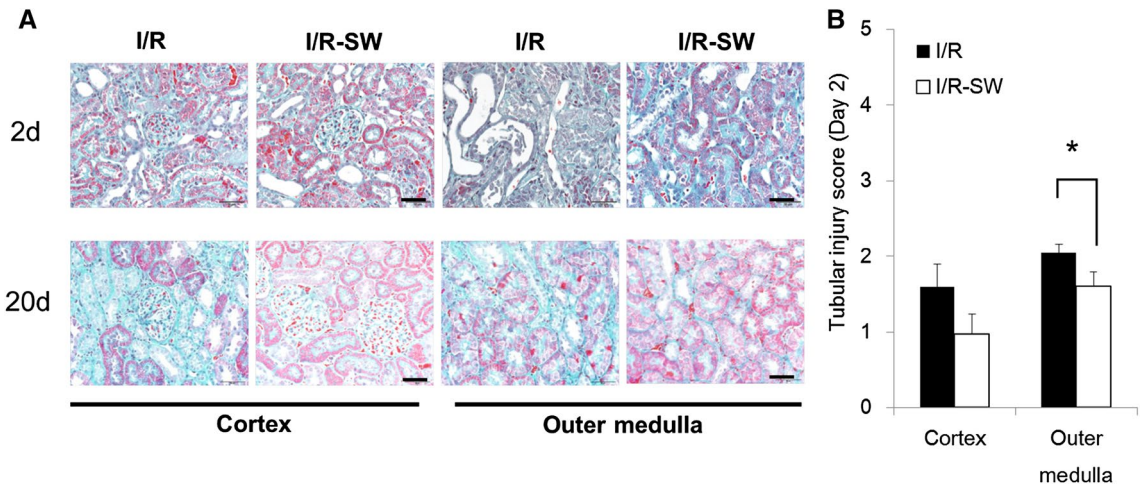

Fig. 3 Histological analyses on day 2 and day 20. **a** Representative photographs of the left (affected side) kidney stained with Elastica-Masson showed prominent renal tubular injury on day 2 (2 days) and day 20 (20 days). Original magnification, ×400. Scale bars represent 50 μm. **b** Renal tubular injury scores for the outer medulla in the I/R-SW group demonstrated a significantly lower score than in the I/R group on day 2. Data are expressed as means ± standard error. Tukey HSD test: $^{*}P < 0.05$. *I/R* ischemia–reperfusion, *SW* shock wave

injury scores tended that I/R-SW was lower than I/R in the cortex and the outer medulla (data not shown); however, there were no significant differences between the I/R and the I/R-SW groups (Fig. 3a). As the right (intact side) kidney retained an almost normal structure on both days 2 and 20, no differences in tubular injury scores for the outer medulla and cortex of the right (intact side) kidney were observed between the I/R-SW and I/R groups (data not shown).

Immunohistochemistry

To determine the extent of original interstitial fibrosis, αSMA immunohistochemistry was performed. On day 2, interstitial αSMA-positive areas surrounded by necrotic tubular epithelium were observed following I/R surgery (Fig. 4a). Although original interstitial fibrosis of both the cortex and outer medulla tended to be less in the I/R-SW group, the percentage of the area was not significantly different compared with the I/R group on day 2. On day 20, the interstitial fibrosis was reduced relative to day 2. However, there were no significant differences between the I/R and the I/R-SW groups (Fig. 4b). ED-1 immunohistochemistry demonstrated macrophage infiltration predominantly adjacent to the outer medullary region (Fig. 4c). The inflammatory cells were all stained with ED-1; however, SW therapy was not found to decrease the number of these cells (Fig. 4d). Cleaved Caspase-3 is a frequently activated protease in cell apoptosis (Fig. 5a). On day 2, SW decreased caspase-3 of the cortex in the left (affected side) kidney on day 2 (I/R-SW vs. I/R (%), 2.52 ± 0.119 vs. 3.17 ± 0.249; $P < 0.05$) (Fig. 5b). Podoplanin-positive lymphatic vessels were observed exclusively in the cortical region in both left (affected side) and right (intact side) kidneys. Lymphatic vessels were not observed in the outer medullary region and the number of vessels in the cortical region was not different between the I/R-SW and SW

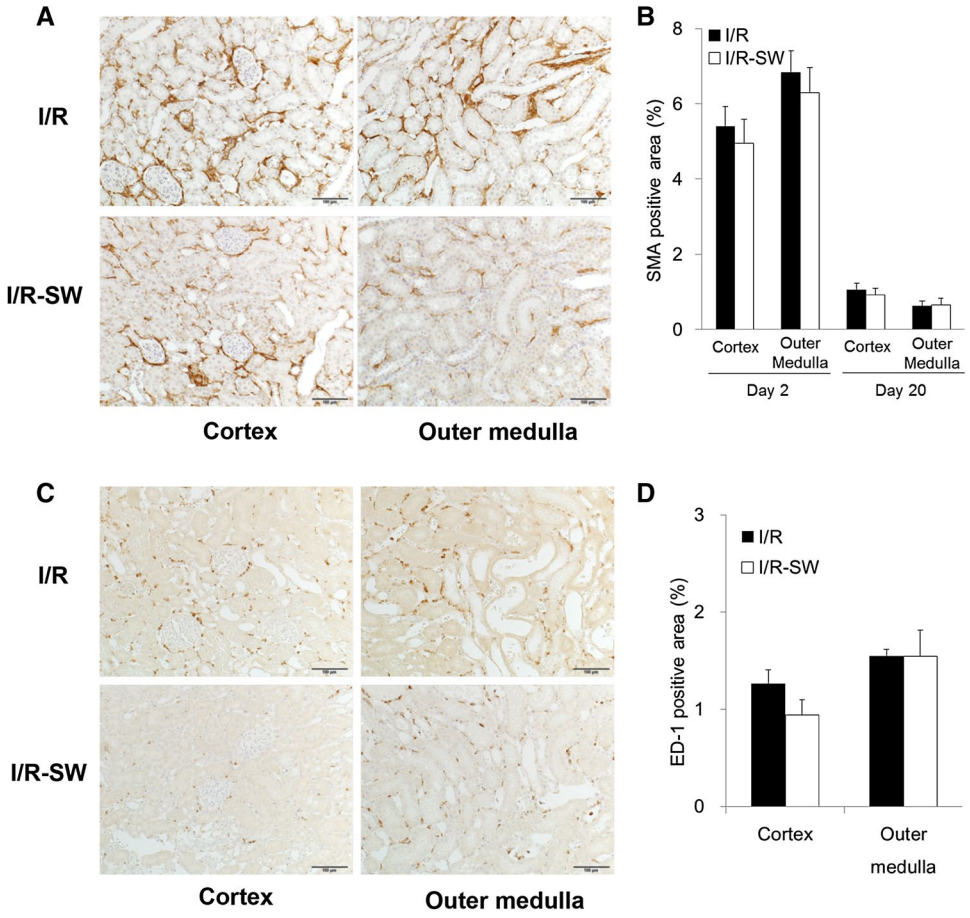

Fig. 4 Immunohistochemical analyses of left (affected side) kidney. Representative photographs of the left (affected side) kidney stained with **a** αSMA and **c** ED-1 antibodies on day 2. Original magnification, ×200. **b** αSMA staining did not demonstrate a significant difference in interstitial fibrosis between the I/R and I/R-SW groups on day 2 and day 20. **d** ED-1 staining did not demonstrate a significant difference in macrophage infiltration around interstitial areas between the I/R and I/R-SW groups on day 2. Data are expressed as means ± standard error. Scale bars represent 100 μm. *I/R* ischemia–reperfusion, *SW* shock wave

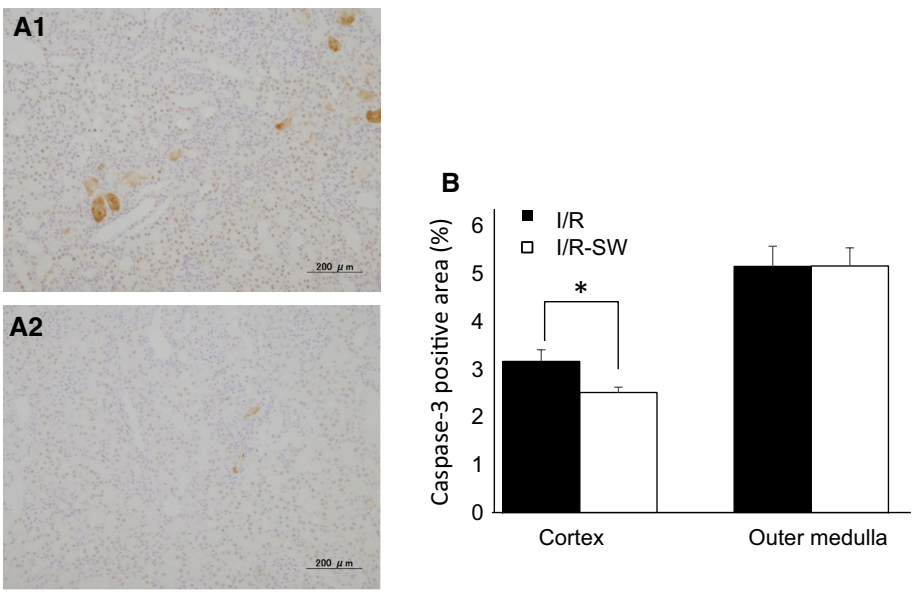

Fig. 5 Immunohistochemical analyses of left (affected side) kidney. Representative photographs stained with Cleaved Caspase-3 antibody on day 2. Each photograph demonstrates **a1** the cortex in the I/R group and **a2** the cortex in the I/R-SW group. Original magnification, ×100. Scale bars represent 200 μm. **b** The Cleaved Caspase-3-positive area in the cortex of the I/R-SW group was significantly decreased compared with the I/R group (*$P < 0.05$). Data are expressed as means ± standard error. Tukey HSD test: *$P < 0.05$. *I/R* ischemia–reperfusion, *SW* shock wave

groups on day 2 (data not shown). Conversely, podoplanin-positive lymphatic vessels were observed in the outer medullary region of the left (affected side) kidney on day 20 (Fig. 6a, b). Additionally, the number of vessels in the left (affected side) outer medullary region of the I/R-SW group was significantly increased compared with the I/R group (I/R-SW vs. I/R, 3.98 ± 0.49 vs. 2.82 ± 0.57/high-power field; $P < 0.05$; Fig. 6c). This phenomenon was not

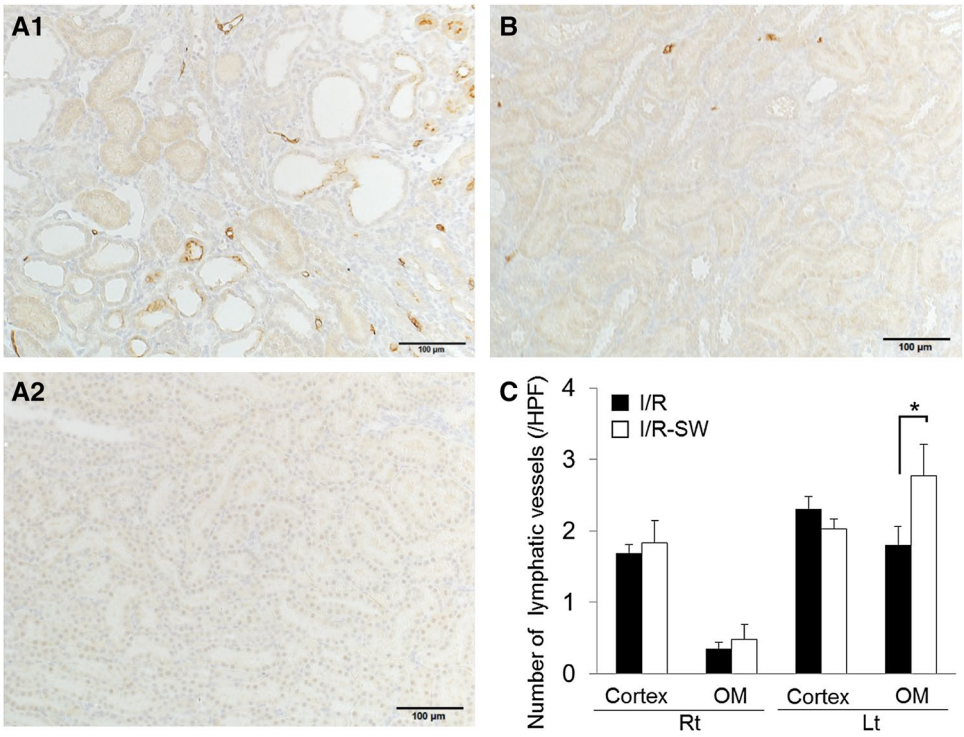

Fig. 6 Immunohistochemical analyses of cortex and outer medulla. Representative photographs stained with podoplanin antibody on day 20. Each photograph demonstrates **a1** the left (affected side) outer medulla in the I/R-SW group, **a2** the right (intact side) outer medulla in the I/R-SW group, and **b** the left (affected side) outer medulla in the I/R group. Original magnification, ×200. Scale bars represent 100 μm. **c** The number of podoplanin-positive lymphatic vessels in the left (affected side) outer medulla of the I/R-SW group was significantly increased compared with the I/R group (*$P < 0.05$). Data are expressed as means ± standard error. Tukey HSD test: *$P < 0.05$. *I/R* ischemia–reperfusion, *SW* shock wave, *Rt* right (intact side) kidney, *Lt* left (affected side) kidney, *OM* outer medulla, *HPF* high-power field

observed in the right (intact side) outer medullary region. To evaluate the angiogenesis, we stained with CD-31 on day 20. However, CD-31-positive vessel was not almost observed and there is no difference between I/R-SW and I/R groups. Therefore, we did not count the vessel (data not shown).

Expression levels of Vegf family members

On day 2, mRNA expression of *Vegf* was upregulated in both left (affected side) and right (intact side) kidneys, except left outer medulla, in the I/R-SW and I/R groups compared with the Sham group (Fig. 7a–d). In particular, SW therapy significantly upregulated *Vegf* expression in the cortex of the right (intact side) kidney in the I/R-SW group compared with the I/R group ($P < 0.05$; Fig. 7a). *Vegf* upregulation was not observed on day 20. The mRNA expression of *Vegf-c* ($P < 0.05$), *Vegfr-3* ($P < 0.05$), and *Vegf-a* ($P < 0.05$) in the right (intact side) cortex was significantly increased in the I/R-SW group compared with the I/R group on day 2 (Fig. 8a–c).

Expression levels of eNOS

eNOS is responsible for most of the vascular NO production. However, the mRNA expression level of eNOS on day 2 varied widely and was not significantly different between the I/R-SW group and I/R group (data not shown).

Discussion

The major findings of the present study are that SW therapy ameliorated tubular injury and improved renal function in a rat model of I/R injury. In addition, increased expression of VEGF family members in the right (intact side) kidney on day 2 and lymphangiogenesis in the left (affected side) kidney on day 20 were observed. These results corroborate the findings of previous studies in other organs described in "Introduction".

Shock wave is based on a longitudinal acoustic wave that propagates through water and soft tissue in a similar manner to ultrasound. SW is a single pressure pulse with a short needle-like positive spike that exerts the cavitation effect

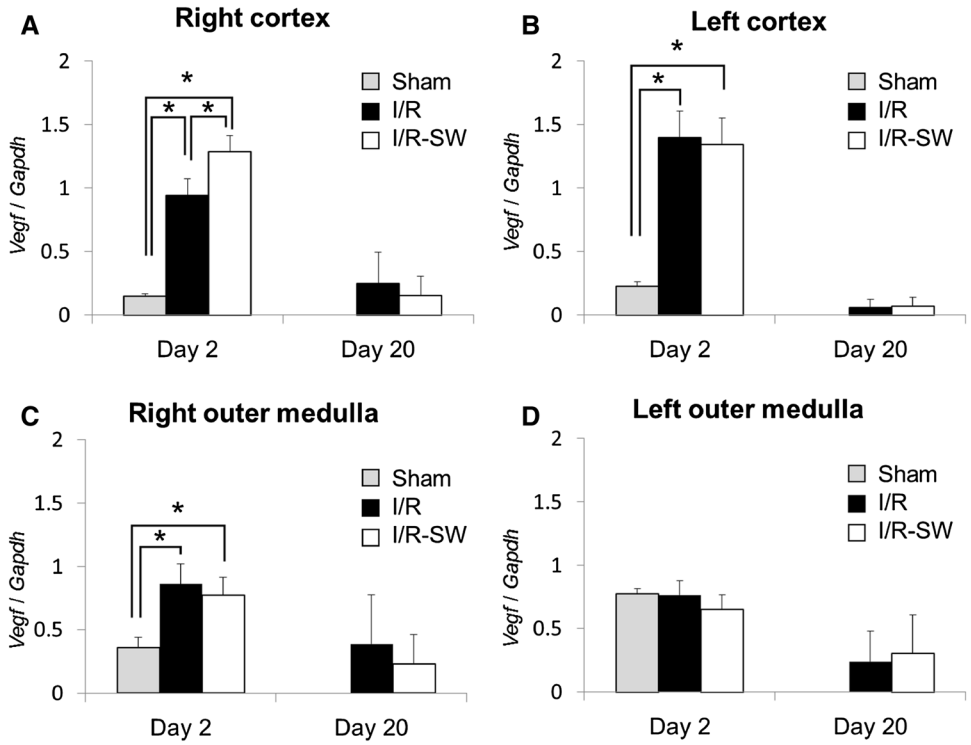

Fig. 7 *Vegf* mRNA expression. **a**–**c** On day 2, Vegf mRNA expression was upregulated in the left (affected side) cortex and right (intact side) kidney in both I/R and I/R-SW groups compared with the Sham group. Particularly in the right (intact side) cortex, mRNA expression was significantly upregulated in the I/R-SW group compared with the I/R group. **d** No difference in Vegf mRNA expression in the left (affected side) outer medulla was observed between three groups. Data are expressed as means ± standard error. Tukey HSD test: $^*P < 0.05$. *I/R* ischemia–reperfusion, *SW* shock wave

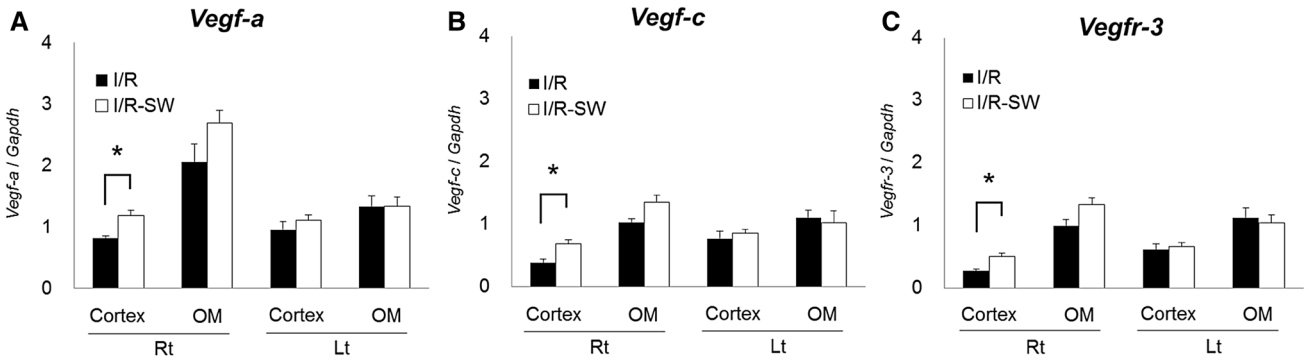

Fig. 8 Expression of *Vegf* family members on day 2. On day 2, right (intact side) cortical mRNA expression levels of **a** *Vegf-a*, **b** *Vegf-c*, and **c** *Vegfr-3* were significantly higher in the I/R-SW group than in the I/R group. Data are expressed as means ± standard error. Tukey HSD test: $^*P < 0.05$, *I/R* ischemia–reperfusion, *SW* shock wave, *Rt* right (intact side) kidney, *Lt* left (affected side) kidney, *OM* outer medulla

and shear stress. The cavitation effect refers to the violent collapse of micrometer-sized bubbles inside and outside the cell [18]. Shear stress on cell surface membranes has been shown to affect the expression of several chemokines and anti-inflammatory cytokines [19]. Although the precise mechanisms for the beneficial effects of SW remain unclear, these effects are regarded as the predominant mechanism underlying the efficacy of SW therapy.

VEGF has several important biological activities in major organs, such as a stimulating angiogenesis, preventing apoptosis, and prompting vascular dilatation through NO. The VEGF family is composed of VEGF-A, VEGF-B, VEGF-C, VEGF-D, placenta-like growth factor (PLGF)-1 and PLGF-2, and three types of receptors, VEGFR-1, VEGFR-2, and VEGFR-3. In the kidney, major sources of VEGF are tubular epithelial cells and podocytes [20], and recent studies showed that renal levels of VEGF are altered in pathologic situations. For example, in a rodent unilateral ureteral obstruction model, decreased VEGF have been shown to have important roles in the progression of renal fibrosis and prevention of angiogenesis [21]. In addition, the previous report demonstrated that administration of VEGF in AKI induced by renal I/R could be a novel potential therapeutic approach [22]. In the report, the rats, which were treated

early with VEGF after I/R, showed the same results as our experiments in the kidney volume and interstitial fibrosis. The mechanism was unknown, but the relationship between the renoprotection and the early upregulation of VEGF after AKI was suggested. In our experiment, it was consistent that VEGF in the contralateral kidney affected and protected the kidney after I/R.

VEGF-C and VEGF-D specifically bind to VEGFR-3 and are predominantly involved in lymphangiogenesis [23]. The renal lymphangiogenesis observed in the present study is a unique finding. The increase in lymphatic vessels has been reported in several conditions, including tumor metastasis, wound healing, and renal transplantation. Such conditions have been shown to induce lymphangiogenesis through the upregulation of VEGF-C and VEGFR-3. Conversely, the role of lymphangiogenesis in renal disorders has yet to be elucidated. Lymphangiogenesis has been demonstrated in a small number of experimental models. A relationship between tubulo-interstitial fibrosis, chronic inflammation, and newly formed lymphatic vessels was demonstrated in a rat remnant kidney model [24]. In addition, changes in kidney weight are key findings in lymphangiogenesis. Classically, it has been believed that intravenous fluid replacement to maintain renal circulation and ameliorate tubular injuries is appropriate in the management of ischemic AKI. However, a new concept has emerged that intravenous fluid replacement raises renal venous pressure, leading to tissue edema, impaired oxygen delivery, and lymphatic drainage [25, 26]. In this study, the upregulation of VEGF improved lymphatic circulation through lymphangiogenesis. Lymphatic circulation might affect improvement of AKI through decreasing renal venous pressure.

The reported expression of VEGF varies between studies on renal I/R models. In the present study, the mRNA expression of *Vegf* family members was increased in the contralateral kidney. Previous studies have reported that VEGF expression is enhanced in a unilateral I/R model [27], while decreased in a bilateral I/R model [28]. These differences may be attributable to the degree of tubular damage.

In the present study, we demonstrated that SW therapy represents a safe and non-invasive technique in renal tissues. SW has been widely used for the treatment of nephrolithiasis as extracorporeal shock wave lithotripsy (ESWL). The renal complications of ESWL include renal and urinary tract obstruction with incomplete stone fragmentation, damage to renal vasculature, renal hematoma, and hematuria. These adverse effects are now believed to be reversible with no long-term effect on renal function [29]. SW therapy in the present study was safe because the energy involved was as low as one-tenth of ESWL. We did not observe any adverse effect during the experiment protocol.

The present study has several limitations. First, the optimal strength and duration of SW have not been completely determined. We previously treated the human umbilical vein endothelial cells (HUVECs) with SW at four energy levels (0, 0.02, 0.09, 0.18, and 0.35 mJ/mm^2) [5]. mRNA expression of *VEGF* on HUVECs was maximum at 0.09 mJ/mm^2. Subsequently, 0.1 mJ/mm^2 has been used safely as SW therapy in many organs [5–13]. We also confirmed that SW of three times per week was effective in a porcine ischemic cardiomyopathy model [5]. Therefore, we treated kidney with 0.1 mJ/mm^2 SW at the same timing in accordance with the previous studies. Second, we selected unilateral I/R model; there was a probability that right (intact side) kidney could compensate renal function. We have performed two experiments to know the best model. We have performed in a bilateral I/R model and the plasma creatinine concentration in the I/R-SW group was not lower than the I/R group on days 2 and 20. We have also performed SW treatment for the Sham rats, and the plasma creatinine concentration was the same with untreated Sham rats on days 2 and 20. These findings showed that SW treatment might not ameliorate too severe renal injury and be ineffective against healthy kidney and we selected the unilateral I/R model. Third, established fibrosis should be irreversible, and, in our examination, the fibrosis area decreased at day 20. We could not explain the reason and it requires further research. Fourth, the mechanisms underlying the efficacy of SW were not fully elucidated. *Vegf* mRNA upregulation only in the contralateral kidney and in the later phase does not necessarily support the evidence that protection of SW therapy is through the stimulation of VEGF family expression and lymphangiogenesis. However, in our study, SW prevented apoptosis in cortex of the left (affected side) kidney and it was suggested that SW was directly effective for the left (affected side) kidney.

Conclusions

We conclude that SW therapy effectively improves renal function in a rodent model of renal I/R injury. This novel and safe technique can be a useful strategy for the clinical management of ischemic AKI.

Compliance with ethical standards

Conflict of interest The authors have declared that no conflicts of interest exist.

Ethical approval The protocols of the present study were approved by the ethics committee on animal experiments of Tohoku University (No. 2011-303).

Informed consent This section is not applicable to this study.

References

1. Yasuda H, Kato A, Fujigaki Y, Hishida A, Shizuoka Kidney Disease Study G. Incidence and clinical outcomes of acute kidney injury requiring renal replacement therapy in Japan. Ther Apher Dial. 2010;14(6):541–6. https://doi.org/10.1111/j.1744-9987.2010.00826.x.
2. Schetz M, Gunst J, De Vlieger G, Van den Berghe G. Recovery from AKI in the critically ill: potential confounders in the evaluation. Intensive Care Med. 2015;41(9):1648–57. https://doi.org/10.1007/s00134-015-3946-3.
3. Chade AR. VEGF: potential therapy for renal regeneration. F1000. Med Rep. 2012;4:1. https://doi.org/10.3410/M4-1.
4. Doi K, Noiri E, Fujita T. Role of vascular endothelial growth factor in kidney disease. Curr Vasc Pharmacol. 2010;8(1):122–8.
5. Nishida T, Shimokawa H, Oi K, Tatewaki H, Uwatoku T, Abe K, et al. Extracorporeal cardiac shock wave therapy markedly ameliorates ischemia-induced myocardial dysfunction in pigs in vivo. Circulation. 2004;110(19):3055–61. https://doi.org/10.1161/01.CIR.0000148849.51177.97.
6. Fukumoto Y, Ito A, Uwatoku T, Matoba T, Kishi T, Tanaka H, et al. Extracorporeal cardiac shock wave therapy ameliorates myocardial ischemia in patients with severe coronary artery disease. Coron Artery Dis. 2006;17(1):63–70.
7. Kikuchi Y, Ito K, Ito Y, Shiroto T, Tsuburaya R, Aizawa K, et al. Double-blind and placebo-controlled study of the effectiveness and safety of extracorporeal cardiac shock wave therapy for severe angina pectoris. Circ J. 2010;74(3):589–91.
8. Serizawa F, Ito K, Kawamura K, Tsuchida K, Hamada Y, Zukeran T, et al. Extracorporeal shock wave therapy improves the walking ability of patients with peripheral artery disease and intermittent claudication. Circ J. 2012;76(6):1486–93.
9. Abe Y, Ito K, Hao K, Shindo T, Ogata T, Kagaya Y, et al. Extracorporeal low-energy shock-wave therapy exerts anti-inflammatory effects in a rat model of acute myocardial infarction. Circ J. 2014;78(12):2915–25.
10. Ito Y, Ito K, Shiroto T, Tsuburaya R, Yi GJ, Takeda M, et al. Cardiac shock wave therapy ameliorates left ventricular remodeling after myocardial ischemia-reperfusion injury in pigs in vivo. Coron Artery Dis. 2010;21(5):304–11.
11. Uwatoku T, Ito K, Abe K, Oi K, Hizume T, Sunagawa K, et al. Extracorporeal cardiac shock wave therapy improves left ventricular remodeling after acute myocardial infarction in pigs. Coron Artery Dis. 2007;18(5):397–404. https://doi.org/10.1097/MCA.0b013e328089f19b.
12. Serizawa F, Ito K, Matsubara M, Sato A, Shimokawa H, Satomi S. Extracorporeal shock wave therapy induces therapeutic lymphangiogenesis in a rat model of secondary lymphoedema. Eur J Vasc Endovasc Surg. 2011;42(2):254–60. https://doi.org/10.1016/j.ejvs.2011.02.029.
13. Yamaya S, Ozawa H, Kanno H, Kishimoto KN, Sekiguchi A, Tateda S, et al. Low-energy extracorporeal shock wave therapy promotes vascular endothelial growth factor expression and improves locomotor recovery after spinal cord injury. J Neurosurg. 2014;121(6):1514–25. https://doi.org/10.3171/2014.8.JNS132562.
14. Gigliotti JC, Huang L, Ye H, Bajwa A, Chattrabhuti K, Lee S, et al. Ultrasound prevents renal ischemia-reperfusion injury by stimulating the splenic cholinergic anti-inflammatory pathway. J Am Soc Nephrol. 2013;24(9):1451–60. https://doi.org/10.1681/asn.2013010084.
15. Gigliotti JC, Huang L, Bajwa A, Ye H, Mace EH, Hossack JA, et al. Ultrasound modulates the splenic neuroimmune axis in attenuating AKI. J Am Soc Nephrol. 2015;26(10):2470–81. https://doi.org/10.1681/asn.2014080769.
16. Roelofs JJ, Rouschop KM, Leemans JC, Claessen N, de Boer AM, Frederiks WM, et al. Tissue-type plasminogen activator modulates inflammatory responses and renal function in ischemia reperfusion injury. J Am Soc Nephrol. 2006;17(1):131–40. https://doi.org/10.1681/ASN.2005010089.
17. Sakamoto I, Ito Y, Mizuno M, Suzuki Y, Sawai A, Tanaka A, et al. Lymphatic vessels develop during tubulointerstitial fibrosis. Kidney Int. 2009;75(8):828–38. https://doi.org/10.1038/ki.2008.661.
18. Apfel RE. Acoustic cavitation: a possible consequence of biomedical uses of ultrasound. Br J Cancer Suppl. 1982;5:140–6.
19. Maisonhaute E, Prado C, White PC, Compton RG. Surface acoustic cavitation understood via nanosecond electrochemistry. Part III: shear stress in ultrasonic cleaning. Ultrason Sonochem. 2002;9(6):297–303.
20. Schrijvers BF, Flyvbjerg A, De Vriese AS. The role of vascular endothelial growth factor (VEGF) in renal pathophysiology. Kidney Int. 2004;65(6):2003–17. https://doi.org/10.1111/j.1523-1755.2004.00621.x.
21. Sun D, Wang Y, Liu C, Zhou X, Li X, Xiao A. Effects of nitric oxide on renal interstitial fibrosis in rats with unilateral ureteral obstruction. Life Sci. 2012;90(23–24):900–9. https://doi.org/10.1016/j.lfs.2012.04.018.
22. Leonard EC, Friedrich JL, Basile DP. VEGF-121 preserves renal microvessel structure and ameliorates secondary renal disease following acute kidney injury. Am J Physiol Ren Physiol. 2008;295(6):F1648-57. https://doi.org/10.1152/ajprenal.00099.2008.
23. Breen EC. VEGF in biological control. J Cell Biochem. 2007;102(6):1358–67. https://doi.org/10.1002/jcb.21579.
24. Matsui K, Nagy-Bojarsky K, Laakkonen P, Krieger S, Mechtler K, Uchida S, et al. Lymphatic microvessels in the rat remnant kidney model of renal fibrosis: aminopeptidase p and podoplanin are discriminatory markers for endothelial cells of blood and lymphatic vessels. J Am Soc Nephrol. 2003;14(8):1981–9.
25. Prowle JR, Echeverri JE, Ligabo EV, Ronco C, Bellomo R. Fluid balance and acute kidney injury. Nat Rev Nephrol. 2010;6(2):107–15. https://doi.org/10.1038/nrneph.2009.213.
26. Prowle JR, Kirwan CJ, Bellomo R. Fluid management for the prevention and attenuation of acute kidney injury. Nat Rev Nephrol. 2014;10(1):37–47. https://doi.org/10.1038/nrneph.2013.232.
27. Bi LY, Zhao DA, Yang DS, Guo JG, Liang B, Zhang RX, et al. Effects of autologous SCF- and G-CSF-mobilized bone marrow stem cells on hypoxia-inducible factor-1 in rats with ischemia-reperfusion renal injury. Genet Mol Res. 2015;14(2):4102–12. https://doi.org/10.4238/2015.April.27.25.
28. Basile DP, Fredrich K, Chelladurai B, Leonard EC, Parrish AR. Renal ischemia reperfusion inhibits VEGF expression and induces ADAMTS-1, a novel VEGF inhibitor. Am J Physiol Ren Physiol. 2008;294(4):F928-36. https://doi.org/10.1152/ajprenal.00596.2007.
29. Labanaris AP, Kuhn R, Schott GE, Zugor V. Perirenal hematomas induced by extracorporeal shock wave lithotripsy (ESWL). Ther Manag Sci World J. 2007;7:1563–6. https://doi.org/10.1100/tsw.2007.236.